JOURNAL OF GUIDANCE, CONTROL, AND DYNAMICS
Vol. 25, No. 1, January–February 2002

Rapid Multitarget Acquisition and Pointing Control of Agile Spacecraft

Bong Wie*
Arizona State University, Tempe, Arizona 85287-6106
and
David Bailey† and Christopher Heiberg‡
Honeywell, Inc., Glendale, Arizona 85308-9650

Study results of developing an attitude control system for agile spacecraft that require rapid retargeting and fast transient settling are presented. In particular, a nonlinear feedback control logic is developed for large-angle, rapid multitarget acquisition and pointing maneuvers subject to various physical constraints, including actuator saturation, slew rate limit, and control bandwidth limit. The rapid multitarget acquisition and pointing capability of the proposed attitude control system is demonstrated for an agile spacecraft equipped with redundant single-gimbal control moment gyros. A realistic case of pointing the line of sight of an imaging satellite in low Earth orbit toward multiple targets on the ground is also briefiy discussed.

I. Introduction

A SPACECRAFT that requires rapid rotational maneuverability or agility is called an agile spacecraft. Such agile spacecraft require an attitude control system that provides rapid multitarget acquisition, pointing, and tracking capabilities.

Future space platforms such as the missile-tracking satellites and the synthetic aperture radar satellites for tracking moving ground targets will, of necessity, require rapid rotational maneuverability or agility. The next-generation commercial Earth-imaging satellites, including the recently launched Ikonos satellite, will also require rapid rotational maneuverability for high-resolution images. Rather than sweep the imaging system from side to side, the whole spacecraft body will turn rapidly. Pointing the entire spacecraft allows the imaging system to achieve a higher definition and improves the resolution for its images. Because the overall cost and effectiveness of such agile spacecraft is greatly affected by the average retargeting time, the development of intelligent control algorithms for rapid retargeting is crucial.

Such rapid retargeting maneuvers are often subjected to the physical limits of actuators, sensors, spacecraft structural rigidity, and other mission constraints. Large-angle slew maneuver logic of most spacecraft, including the recently flown Clementine spacecraft, is often driven by wheel momentum as well as torque saturation, but not by sensors. On the other hand, the rest-to-rest slew control problem of the x-ray timing explorer (XTE) spacecraft is mainly driven by the slew rate constraint caused by the saturation limit of low-rate gyros. The angular momentum change of the XTE spacecraft during its planned slew maneuvers is well within its wheel momentum saturation limit. For certain missions, it may also be necessary to maintain rotation about an inertially fixed axis during an acquisition mode so that a particular sensor can pick up a particular target.

In particular, when control moment gyros (CMGs) are employed as primary actuators because of their much higher control torque capability of 100–5000 N · m maximum torque compared with reaction wheels with 1–2 N · m maximum torque, the CMG singularity problem becomes one of the major constraints on the maneuverability of such agile spacecraft. When agile spacecraft are controlled by CMGs, momentum saturation, singularity avoidance, and gimbal rate saturation need to be further considered in developing an attitude control system for large-angle, rapid multitarget acquisition and pointing maneuvers.

In this paper, expanding on the previous work in Refs. 1–4, we further develop a nonlinear feedback control logic for rapid retargeting control of agile spacecraft subject to various physical constraints, including actuator saturation, slew rate limit, control bandwidth limit, and/or eigenaxis slew constraints.

The remainder of this paper is organized as follows. In Sec. II, a single-axis attitude control problem is described to illustrate the proposed nonlinear control algorithm of achieving rapid, large-angle retargeting and fast transient settling in the presence of the actuator saturation and slew rate limit. Section III is a numerical example of this. In Sec. IV a three-axis quaternion feedback control problem is described, and the nonlinear control algorithm illustrated in Sec. II is extended to the three-axis attitude control problem. In Sec. V the proposed nonlinear control logic is applied to a rapid, retargeting control problem of an agile spacecraft equipped with redundant single-gimbal CMGs. In Sec. VI, a more realistic case of pointing the line of sight of an imaging satellite in low Earth orbit toward multiple targets on the ground is also briefiy discussed. This complex problem was the main motivation for developing the proposed nonlinear control logic.

II. Single-Axis Attitude Control

For the purpose of illustrating the proposed nonlinear feedback control logic, consider the single-axis attitude control problem of a rigid spacecraft described by

$$J\ddot{\theta} = u, \qquad |u(t)| \le U \tag{1}$$

where J is the spacecraft moment of inertia, θ the attitude angle, and u the control torque input with the saturation limit of $\pm U$.

The time-optimal feedback control logic for the commanded constant attitude angle of θ_c is given by[5]

$$u = -U\,\mathrm{sgn}[e + (1/2a)\dot{\theta}|\dot{\theta}|] \tag{2}$$

where $e = \theta - \theta_c$ and $a = U/J$ is the maximum control acceleration. The signum function is defined as $\mathrm{sgn}(x) = 1$ if $x > 0$ and $\mathrm{sgn}(x) = -1$ if $x < 0$.

In practice, a direct implementation of such an ideal, time-optimal switching control logic results in a chattering problem. Consequently, there exist various ways of avoiding such a chattering

Received 13 April 2000; revision received 22 February 2001; accepted for publication 1 April 2001.

*Professor, Department of Mechanical and Aerospace Engineering; bong.wie@asu.edu. Associate Fellow AIAA.
†Principal Fellow, Satellite Systems Operation; dbailey@az76.honeywell.com. Member AIAA.
‡Staff Engineer, Satellite Systems Operation; cheiberg@az76.honeywell.com. Member AIAA.

problem inherent in the ideal, time-optimal switching control logic. Consider a feedback control logic of the form

$$u = -\underset{U}{\text{sat}}\left\{K\underset{L}{\text{sat}}(e) + C\dot{\theta}\right\} \tag{3}$$

where $e = \theta - \theta_c$ and K and C are, respectively, the attitude and attitude rate gains to be properly determined. The saturation function is defined as

$$\underset{L}{\text{sat}}(e) = \begin{cases} L & \text{if} \quad e \geq L \\ e & \text{if} \quad |e| < L \\ -L & \text{if} \quad e \leq -L \end{cases} \tag{4}$$

and it can also be represented as

$$\underset{L}{\text{sat}}(e) = \text{sgn}(e)\min\{|e|, L\} \tag{5}$$

Because of the presence of a limiter in the attitude-error feedback loop, the attitude rate becomes constrained as

$$-|\dot{\theta}|_{\max} \leq \dot{\theta} \leq |\dot{\theta}|_{\max} \tag{6}$$

where $|\dot{\theta}|_{\max} = LK/C$. For most practical cases, a proper use of the feedback control logic (3) will result in a typical bang-off-bang control.

For the nominal range of attitude-error signals that do not saturate the actuator, the controller gains, $K = kJ$ and $C = cJ$, can be determined such that

$$k = \omega_n^2, \qquad c = 2\zeta\omega_n \tag{7}$$

where ω_n and ζ are, respectively, the desired or specified linear control bandwidth and damping ratio. Furthermore, if the maximum slew rate is specified as $|\dot{\theta}|_{\max}$, then the limiter in the attitude-error feedback loop can be selected simply as

$$L = (C/K)|\dot{\theta}|_{\max} = (c/k)|\dot{\theta}|_{\max} \tag{8}$$

However, as the attitude-error signal gets larger, and also as the slew rate limit becomes larger for rapid maneuvers, the overall response becomes sluggish with increased transient overshoot because of the actuator saturation. To achieve rapid transient settlings even for large commanded attitude angles, the slew rate limit needs to be adjusted as developed in Ref. 6, as follows:

$$|\dot{\theta}|_{\max} = \min\left\{\sqrt{2a|e|},\ |\omega|_{\max}\right\} \tag{9}$$

where $e = \theta - \theta_c$ is the attitude error, $|\omega|_{\max}$ is the specified maximum slew rate, and $a = U/J$ is the maximum control acceleration. A smaller value than the nominal a is to be used to accommodate various uncertainties in the spacecraft inertia and actuator dynamics.

Such a variable limiter in the attitude-error feedback loop has the self-adjusting saturation limit,

$$L = (C/K)|\dot{\theta}|_{\max} = (c/k)|\dot{\theta}|_{\max} = (c/k)\min\left\{\sqrt{2a|e|},\ |\omega|_{\max}\right\} \tag{10}$$

and we obtain a nonlinear control logic of the form

$$u = -\underset{U}{\text{sat}}\left\{K\underset{L}{\text{sat}}(e) + C\dot{\theta}\right\} = -\underset{U}{\text{sat}}\left\{kJ\,\text{sgn}(e)\min\left[|e|, (c/k)\sqrt{2a|e|}, (c/k)|\omega|_{\max}\right] + cJ\dot{\theta}\right\} \tag{11}$$

If an integral control is necessary to eliminate a steady-state pointing error due to any constant external disturbance, the feedback control logic (11) can be further modified into the following proportional–integral–derivative (PID) saturation control logic,

$$u = -\underset{U}{\text{sat}}\left\{K\underset{L}{\text{sat}}\left(e + \frac{1}{T}\int e\right) + C\dot{\theta}\right\} \tag{12}$$

where T is the time constant of integral control and L is given by Eq. (10). In terms of the standard notation for PID controller gains, K_P, K_I, and K_D, we have

$$K_P = K, \qquad K_I = K/T, \qquad K_D = C \tag{13}$$

The PID controller gains can be determined as

$$K_P = J\left(\omega_n^2 + 2\zeta\omega_n/T\right) \tag{14a}$$

$$K_I = J\left(\omega_n^2/T\right) \tag{14b}$$

$$K_D = J(2\zeta\omega + 1/T) \tag{14c}$$

and the time constant T of integral control is often selected as $T \approx 10/(\zeta\omega_n)$.

If the attitude reference input to be tracked is a smooth function, instead of a multistep input, we may employ a PID saturation control logic of the following form:

$$u = -\underset{U}{\text{sat}}\left\{kJ\,\underset{L}{\text{sat}}\left(e + \frac{1}{T}\int e\right) + cJ\dot{e}\right\} \tag{15}$$

where $e = \theta - \theta_c$.

Also note that the equivalent single-axis representation of the quaternion-error feedback control logic to be described in Sec. IV is given by

$$u = -\underset{U}{\text{sat}}\left\{2kJ\,\underset{L}{\text{sat}}\left(e + \frac{1}{T}\int e\right) + cJ\dot{\theta}\right\} \tag{16}$$

where $e = \sin\frac{1}{2}(\theta - \theta_c)$ and

$$L = (c/2k)|\dot{\theta}|_{\max} = (c/2k)\min\left\{\sqrt{4a|e|}, |\omega|_{\max}\right\} \tag{17}$$

For a PID-type saturation control logic of form (12), (15), or (16), the so-called integrator antiwindup or integrator synchronization is necessary to avoid the phenomenon known as integrator windup, inherent in all PID-type controllers with actuator saturation.[7,8] Such integrator windup results in substantial transient overshoot and control effort. If the controller is implemented on a digital computer, integrator antiwindup can be simply achieved by turning off the integral action as soon as the actuator or any other limiter in the control loop saturates.

III. Numerical Example

Consider the single-axis attitude control problem of a flexible spacecraft with colocated actuator and sensor, described by the transfer function

$$\frac{\theta(s)}{u(s)} = \frac{1}{Js^2}\frac{s^2/\omega_z^2 + 1}{s^2/\omega_p^2 + 1} \tag{18}$$

The nominal spacecraft parameters are assumed as $J = 21{,}400\ \text{kg}\cdot\text{m}^2$, $\omega_z = 5$ rad/s, and $\omega_p = 6$ rad/s. For simplicity, only one dominant flexible mode is included. Actuator dynamics is assumed as

$$u/u_c = (50)^2/[s^2 + 2(0.7)(50)s + (50)^2] \tag{19}$$

where u is the actual control torque acting on the spacecraft and u_c is the control torque command with the saturation limit of $\pm 1000\ \text{N}\cdot\text{m}$. A PID saturation feedback control logic of form (12) is considered.

Assuming $\omega_n = 3$ rad/s, $\zeta = 0.9$, and $T = 10$ s, we can determine the controller gains $K = kJ$ and $C = cJ$ as

$$k = \omega_n^2 + 2\zeta\omega_n/T = 9.54, \qquad c = 2\zeta\omega_n + 1/T = 5.5$$

Commanded attitude angles for two successive rest-to-rest maneuvers are assumed as $\theta_c = 10$ deg for $0 \leq t < 20$ s and $\theta_c = 50$ deg for $t \geq 20$ s.

Simulation results for the following two controllers are compared in Figs. 1 and 2. Equations (20a) and (20b) represent controllers 1 and 2, respectively,

$$u_c = -\underset{U}{\text{sat}}\left\{kJ\left(e + \frac{1}{T}\int e\right) + cJ\dot{\theta}\right\} \tag{20a}$$

$$u_c = -\underset{U}{\text{sat}}\left\{kJ\,\underset{L}{\text{sat}}\left(e + \frac{1}{T}\int e\right) + cJ\dot{\theta}\right\} \tag{20b}$$

$$L = (c/k)\min\left\{\sqrt{2a|e|}, |\omega|_{\max}\right\} \tag{20c}$$

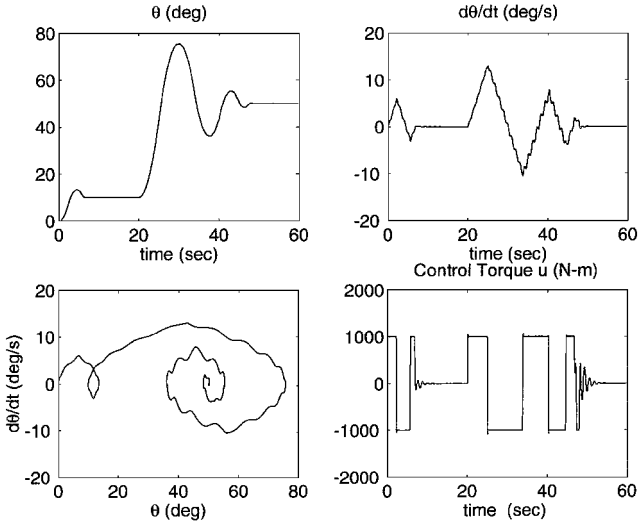

Fig. 1 Simulation results of the standard PID saturation control logic without variable limiter L (controller 1).

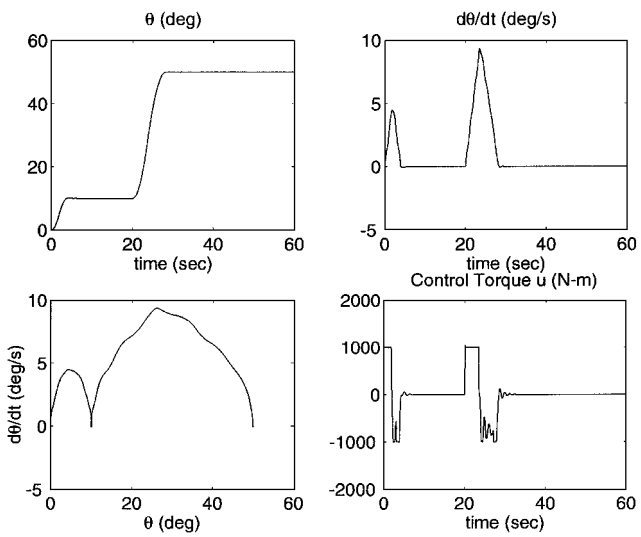

Fig. 2 Simulation results of the constant-gain PID saturation control logic with variable limiter L (controller 2).

where $e = \theta - \theta_c$. The maximum slew rate is assumed as $|\omega|_{\max} = 10$ deg/s for controller 2. The maximum control acceleration a is chosen as 70% of U/J to accommodate the actuator dynamics as well as the control acceleration uncertainty.

Figure 1 shows the simulation results for controller 1; the sluggish response with excessive transient overshoot caused by the actuator saturation is evident for the large commanded attitude angle of 50 deg. As shown in Fig. 2, however, the rapid retargeting capability (without excessive transient overshoot) of the proposed constant-gain, PID-type control system with the variable limiter L is demonstrated.

IV. Three-Axis Quaternion Feedback Control

In this section, a three-axis quaternion feedback control problem is described, and the nonlinear control algorithm illustrated in Sec. II is extended to the three-axis attitude control problem.

A. Quaternion Feedback Control Logic

Consider the rotational equations of motion of a rigid spacecraft described by

$$\boldsymbol{J}\dot{\boldsymbol{\omega}} + \boldsymbol{\omega} \times \boldsymbol{J}\boldsymbol{\omega} = \boldsymbol{u} \tag{21}$$

where $\boldsymbol{J}$ is the inertia matrix, $\boldsymbol{\omega} = (\omega_1, \omega_2, \omega_3)$ the angular velocity vector, and $\boldsymbol{u} = (u_1, u_2, u_3)$ the control torque input vector. The cross product of two vectors is represented in matrix notation as

$$\boldsymbol{\omega} \times \boldsymbol{h} \equiv \begin{bmatrix} 0 & -\omega_3 & \omega_2 \\ \omega_3 & 0 & -\omega_1 \\ -\omega_2 & \omega_1 & 0 \end{bmatrix} \begin{bmatrix} h_1 \\ h_2 \\ h_3 \end{bmatrix} \tag{22}$$

where $\boldsymbol{h} = \boldsymbol{J}\boldsymbol{\omega}$ is the angular momentum vector. It is assumed that the angular velocity vector components ω_i along the body-fixed control axes are measured by rate gyros.

Let a unit vector along the Euler axis be denoted by $\boldsymbol{\lambda} = (\lambda_1, \lambda_2, \lambda_3)$ where λ_i are the direction cosines of the Euler axis relative to either an inertial reference frame or the body-fixed control axes. The four elements of quaternions are then defined as

$$q_1 = \lambda_1 \sin(\theta/2) \tag{23a}$$

$$q_2 = \lambda_2 \sin(\theta/2) \tag{23b}$$

$$q_3 = \lambda_3 \sin(\theta/2) \tag{23c}$$

$$q_4 = \cos(\theta/2) \tag{23d}$$

where θ denotes the rotation angle about the Euler axis, and we have $q_1^2 + q_2^2 + q_3^2 + q_4^2 = 1$.

The quaternion kinematic direrential equations are given by

$$\begin{bmatrix} \dot{q}_1 \\ \dot{q}_2 \\ \dot{q}_3 \\ \dot{q}_4 \end{bmatrix} = \frac{1}{2} \begin{bmatrix} 0 & \omega_3 & -\omega_2 & \omega_1 \\ -\omega_3 & 0 & \omega_1 & \omega_2 \\ \omega_2 & -\omega_1 & 0 & \omega_3 \\ -\omega_1 & -\omega_2 & -\omega_3 & 0 \end{bmatrix} \begin{bmatrix} q_1 \\ q_2 \\ q_3 \\ q_4 \end{bmatrix} \tag{24}$$

Similar to the Euler-axis vector $\boldsymbol{\lambda} = (\lambda_1, \lambda_2, \lambda_3)$, define a quaternion vector $\boldsymbol{q} = (q_1, q_2, q_3)$ such that

$$\boldsymbol{q} = \boldsymbol{\lambda} \sin(\theta/2) \tag{25}$$

Note that in this paper the vector part of the quaternions, denoted by $\boldsymbol{q} = (q_1, q_2, q_3)$, is simply called the quaternion vector. Then, Eq. (24) can be rewritten as

$$\dot{\boldsymbol{q}} = -\tfrac{1}{2}\boldsymbol{\omega} \times \boldsymbol{q} + \tfrac{1}{2} q_4 \boldsymbol{\omega} \tag{26a}$$

$$\dot{q}_4 = -\tfrac{1}{2}\boldsymbol{\omega}^T \boldsymbol{q} \tag{26b}$$

where

$$\boldsymbol{\omega} \times \boldsymbol{q} \equiv \begin{bmatrix} 0 & -\omega_3 & \omega_2 \\ \omega_3 & 0 & -\omega_1 \\ -\omega_2 & \omega_1 & 0 \end{bmatrix} \begin{bmatrix} q_1 \\ q_2 \\ q_3 \end{bmatrix} \tag{27}$$

Because quaternions are well suited for onboard real-time computation, spacecraft orientation is now commonly described in terms of the quaternions, and a linear state-feedback controller of the following form can be considered for real-time implementation:

$$\boldsymbol{u} = -\boldsymbol{K}\boldsymbol{q} - \boldsymbol{C}\boldsymbol{\omega} \tag{28}$$

where $\boldsymbol{K}$ and $\boldsymbol{C}$ are controller gain matrices to be properly determined.

If the commanded attitude quaternion vector is given as $\boldsymbol{q}_c = (q_{1c}, q_{2c}, q_{3c})$, then the control logic (28) can be simply modified into the following form:

$$\boldsymbol{u} = -\boldsymbol{K}\boldsymbol{e} - \boldsymbol{C}\boldsymbol{\omega} \tag{29}$$

where $\boldsymbol{e} = (e_1, e_2, e_3)$ is called the attitude-error vector. The commanded attitude quaternions $(q_{1c}, q_{2c}, q_{3c}, q_{4c})$ and the current attitude quaternions (q_1, q_2, q_3, q_4) are related to the attitude-error quaternions (e_1, e_2, e_3, e_4) as follows:

$$\begin{bmatrix} e_1 \\ e_2 \\ e_3 \\ e_4 \end{bmatrix} = \begin{bmatrix} q_{4c} & q_{3c} & -q_{2c} & -q_{1c} \\ -q_{3c} & q_{4c} & q_{1c} & -q_{2c} \\ q_{2c} & -q_{1c} & q_{4c} & -q_{3c} \\ q_{1c} & q_{2c} & q_{3c} & q_{4c} \end{bmatrix} \begin{bmatrix} q_1 \\ q_2 \\ q_3 \\ q_4 \end{bmatrix} \tag{30}$$

It was shown in Refs. 1 and 2 that the closed-loop nonlinear system of a rigid spacecraft with the linear state-feedback controller of the form (28) or (29) is globally asymptotically stable for the following gain selections: 1) controller 1: $\boldsymbol{K} = 2k\boldsymbol{I}$, $\boldsymbol{C} = \text{diag}(c_1, c_2, c_3)$; 2) controller 2: $\boldsymbol{K} = (2k/q_4^3)\boldsymbol{I}$, $\boldsymbol{C} = \text{diag}(c_1, c_2, c_3)$; 3) controller 3: $\boldsymbol{K} = 2k\ \text{sgn}(q_4)\boldsymbol{I}$, $\boldsymbol{C} = \text{diag}(c_1, c_2, c_3)$; and 4) controller 4: $\boldsymbol{K} = [\alpha\boldsymbol{J} + \beta\boldsymbol{I}]^{-1}, \boldsymbol{K}^{-1}\boldsymbol{C} > 0$, where k and c_i are positive scalar constants, $\boldsymbol{I}$ is a 3×3 identity matrix, $\text{sgn}(\cdot)$ denotes the signum function, and α and β are nonnegative scalars. Note that controller 1 is a special case of controller 4 and that β can be selected as zero when $\alpha \neq 0$. Controllers 2 and 3 approach the origin, either $(0, 0, 0, +1)$ or $(0, 0, 0, -1)$, by taking a shorter angular path.

B. Eigenaxis Rotation

The gyroscopic term of Euler's rotational equation of motion is not significant for most practical rotational maneuvers. However, in some cases, it may be desirable to directly counteract the term by control torque as

$$\boldsymbol{u} = -\boldsymbol{K}\boldsymbol{e} - \boldsymbol{C}\boldsymbol{\omega} + \boldsymbol{\omega} \times \boldsymbol{J}\boldsymbol{\omega} \tag{31}$$

It was shown in Ref. 2 that the closed-loop system with the controller (31) is globally asymptotically stable if the matrix $\boldsymbol{K}^{-1}\boldsymbol{C}$ is positive definite. A natural selection of $\boldsymbol{K}$ and $\boldsymbol{C}$ for guaranteeing such condition is $\boldsymbol{K} = 2k\boldsymbol{J}$ and $\boldsymbol{C} = c\boldsymbol{J}$, where k and c are positive scalar constants to be properly selected. We often choose k and c as $k \approx \omega_n^2$ and $c \approx 2\zeta\omega_n$, where ω_n and ζ are, respectively, the desired or specified linear control bandwidth and damping ratio of the three-axis attitude control system.

Furthermore, a rigid spacecraft with the controller

$$\boldsymbol{u} = -\boldsymbol{J}(2k\boldsymbol{e} + c\boldsymbol{\omega}) + \boldsymbol{\omega} \times \boldsymbol{J}\boldsymbol{\omega} \tag{32}$$

performs a rest-to-rest reorientation maneuver about an eigenaxis along the commanded quaternion vector $\boldsymbol{q}_c$.

An integral control, if needed, can also be added to the quaternion-error feedback control logic (32), as follows:

$$\boldsymbol{u} = -\boldsymbol{J}\left(2k\boldsymbol{e} + \frac{2k}{T}\int \boldsymbol{e} + c\boldsymbol{\omega}\right) + \boldsymbol{\omega} \times \boldsymbol{J}\boldsymbol{\omega} \tag{33}$$

where T is the time constant of quaternion-error integral control. Because the gyroscopic decoupling control term, $\boldsymbol{\omega} \times \boldsymbol{J}\boldsymbol{\omega}$, of Eq. (33) is not needed for most practical rotational maneuvers, the term will not be considered in the remainder of this paper.

C. Cascade-Saturation Control Logic

Consider the rotational equations of motion of a rigid spacecraft described by

$$\dot{\boldsymbol{q}} = \boldsymbol{f}(\boldsymbol{q}, \boldsymbol{\omega}) = -\tfrac{1}{2}\boldsymbol{\omega} \times \boldsymbol{q} \pm \tfrac{1}{2}\sqrt{1 - \|\boldsymbol{q}\|^2}\,\boldsymbol{\omega} \tag{34a}$$

$$\dot{\boldsymbol{\omega}} = \boldsymbol{g}(\boldsymbol{\omega}, \boldsymbol{u}) = \boldsymbol{J}^{-1}(-\boldsymbol{\omega} \times \boldsymbol{J}\boldsymbol{\omega} + \boldsymbol{u}) \tag{34b}$$

where $\boldsymbol{J}$ is the inertia matrix, $\boldsymbol{q} = (q_1, q_2, q_3)$ is the quaternion vector, $\boldsymbol{\omega} = (\omega_1, \omega_2, \omega_3)$ is the angular velocity vector, $\boldsymbol{u} = (u_1, u_2, u_3)$ is the control input vector, and

$$\|\boldsymbol{q}\|^2 \equiv \boldsymbol{q}^T\boldsymbol{q} = q_1^2 + q_2^2 + q_3^2 \tag{35}$$

The state vector of the system, denoted by $\boldsymbol{x}$, is then defined as

$$\boldsymbol{x} = \begin{bmatrix} \boldsymbol{q} \\ \boldsymbol{\omega} \end{bmatrix} \tag{36}$$

A dynamic system described by a set of differential equations of the form (34) is called a cascaded system because $\boldsymbol{q}$ does not appear in Eq. (34b). Saturation functions employed for the cascade-saturation controller can be defined as follows.

A saturation function of an n-dimensional vector $\boldsymbol{x} = (x_1, \ldots, x_n)$ is defined as

$$\underset{L_i}{\text{sat}}(\boldsymbol{x}) = \begin{bmatrix} \text{sat}_{L_1}(x_1) \\ \text{sat}_{L_2}(x_2) \\ \vdots \\ \text{sat}_{L_n}(x_n) \end{bmatrix} \tag{37}$$

Similarly, a signum function of an n-dimensional vector $\boldsymbol{x}$ is defined as

$$\text{sgn}(\boldsymbol{x}) = \begin{bmatrix} \text{sgn}(x_1) \\ \text{sgn}(x_2) \\ \vdots \\ \text{sgn}(x_n) \end{bmatrix} \tag{38}$$

A normalized saturation function of an n-dimensional vector $\boldsymbol{x}$ is defined as

$$\underset{U}{\text{sat}}(\boldsymbol{x}) = \begin{cases} \boldsymbol{x} & \text{if} \quad \mu(\boldsymbol{x}) < U \\ \boldsymbol{x}[U/\mu(\boldsymbol{x})] & \text{if} \quad \mu(\boldsymbol{x}) \geq U \end{cases} \tag{39}$$

where $\mu(\boldsymbol{x})$ is a positive scalar function of $\boldsymbol{x}$ that characterizes the largeness of the vector $\boldsymbol{x}$.

Because the largeness of a vector $\boldsymbol{x}$ is often characterized by its norms, we may choose $\mu(\boldsymbol{x}) = \|\boldsymbol{x}\|_2 = \sqrt{(\boldsymbol{x}^T\boldsymbol{x})}$ or $\mu(\boldsymbol{x}) = \|\boldsymbol{x}\|_\infty = \max\{x_1, \ldots, x_n\}$ Note that the normalized saturation of a vector $\boldsymbol{x}$, as defined earlier, has the same direction of the vector $\boldsymbol{x}$ itself before saturation, that is, it maintains the direction of the vector.

A state-feedback controller of the following form is called the m-layer cascade-saturation controller,

$$\boldsymbol{u} = \boldsymbol{Q}_m \underset{U}{\text{sat}}\Big\{\boldsymbol{P}_m\boldsymbol{x} + \cdots + \boldsymbol{Q}_2 \text{sat}\Big[\boldsymbol{P}_2\boldsymbol{x} + \boldsymbol{Q}_1 \underset{L_i}{\text{sat}}(\boldsymbol{P}_1\boldsymbol{x})\Big]\Big\} \tag{40}$$

where $\boldsymbol{P}_i$ and $\boldsymbol{Q}_i$ are the controller gain matrices to be properly determined. If $\boldsymbol{Q}_i$ and $\boldsymbol{P}_i$ are diagonal matrices, then we have an m-layer decentralized cascade-saturation controller. The simplest form of a two-layer cascade-saturation control logic for a rigid spacecraft can be expressed as[3,4]

$$\boldsymbol{u} = -\underset{U}{\text{sat}}\Big[\boldsymbol{P}\boldsymbol{\omega} + \boldsymbol{Q}\underset{L_i}{\text{sat}}(\boldsymbol{q})\Big] \tag{41}$$

D. Slew Rate Limit and Control Input Saturation

Consider a rigid spacecraft that is required to maneuver about an inertially fixed axis as fast as possible, but not exceeding the specified maximum slew rate about that eigenaxis. The following saturation control logic provides such a rest-to-rest eigenaxis rotation under slew rate constraint[3,4]

$$\begin{aligned} \boldsymbol{u} &= -\boldsymbol{K}\underset{L_i}{\text{sat}}\left(\boldsymbol{e} + \frac{1}{T}\int \boldsymbol{e}\right) - \boldsymbol{C}\boldsymbol{\omega} \\ &= -\boldsymbol{J}\left\{2k\underset{L_i}{\text{sat}}\left(\boldsymbol{e} + \frac{1}{T}\int \boldsymbol{e}\right) + c\boldsymbol{\omega}\right\} \end{aligned} \tag{42}$$

where $\boldsymbol{e} = (e_1, e_2, e_3)$ is the quaternion-error vector, $\boldsymbol{K} = 2k\boldsymbol{J}$, $\boldsymbol{C} = c\boldsymbol{J}$, and the saturation limits L_i are determined as

$$L_i = (c/2k)|\omega_i|_{\max} \tag{43}$$

where $|\omega_i|_{\max}$ is the specified maximum angular rate about each axis.

Assume that the control torque input for each axis is constrained as

$$-U \leq u_i(t) \leq +U, \qquad i = 1, 2, 3 \tag{44}$$

where U is the saturation limit of each control input. Then, a control logic that accommodates possible control torque input saturation but

that still provides an eigenaxis rotation under slew rate constraint can be expressed as

$$\boldsymbol{\tau} = -\boldsymbol{J}\left\{2k \underset{L_i}{\text{sat}}\left(\boldsymbol{e} + \frac{1}{T}\int \boldsymbol{e}\right) + c\boldsymbol{\omega}\right\} \tag{45}$$

$$\boldsymbol{u} = \underset{U}{\text{sat}}(\boldsymbol{\tau}) = \begin{cases} \boldsymbol{\tau} & \text{if} \quad \|\boldsymbol{\tau}\|_\infty < U \\ U(\boldsymbol{\tau}/\|\boldsymbol{\tau}\|_\infty) & \text{if} \quad \|\boldsymbol{\tau}\|_\infty \geq U \end{cases} \tag{46}$$

where $\|\boldsymbol{\tau}\|_\infty = \max\{|\tau_1|, |\tau_2|, |\tau_3|\}$.

Similar to the case of single-axis attitude control discussed in Sec. I for achieving rapid transient settlings for large attitude-error signals, the slew rate limit is adjusted as

$$L_i = (c/2k)\min\left\{\sqrt{4a_i|e_i|}, |\omega_i|_{\max}\right\} \tag{47}$$

where $a_i = U/J_{ii}$ is the maximum control acceleration about the ith control axis and where $|\omega_i|_{\max}$ is the specified maximum angular rate about each axis.

E. Simulation Results

Consider the three-axis attitude control problem of a rigid spacecraft with the following nominal inertia matrix in units of kg · m^2:

$$\boldsymbol{J} = \begin{bmatrix} 21{,}400 & 2100 & 1800 \\ 2100 & 20{,}100 & 500 \\ 1800 & 500 & 5000 \end{bmatrix} \tag{48}$$

Actuator dynamics in each axis is assumed as

$$u_i/u_{ic} = (50)^2/[s^2 + 2(0.7)(50)s + (50)^2] \tag{49}$$

where u_i is the actual control torque acting along the ith control axis of the spacecraft and u_{ic} is the control torque command with the saturation limit of ± 1000 N · m.

The proposed three-axis control logic is then given by

$$\boldsymbol{\tau} = -\boldsymbol{J}\left\{2k \underset{L_i}{\text{sat}}\left(\boldsymbol{e} + \frac{1}{T}\int \boldsymbol{e}\right) + c\boldsymbol{\omega}\right\} \tag{50}$$

where $\boldsymbol{e}$ is the quaternion-error vector and

$$L_i = (c/2k)\min\left\{\sqrt{4a_i|e_i|}, |\omega_i|_{\max}\right\} \tag{51}$$

$$\boldsymbol{u} = \underset{U}{\text{sat}}(\boldsymbol{\tau}) = \begin{cases} \boldsymbol{\tau} & \text{if} \quad \|\boldsymbol{\tau}\|_\infty < U \\ U(\boldsymbol{\tau}/\|\boldsymbol{\tau}\|_\infty) & \text{if} \quad \|\boldsymbol{\tau}\|_\infty \geq U \end{cases} \tag{52}$$

Assuming $\omega_n = 3$ rad/s, $\zeta = 0.9$, and $T = 10$ s, we can determine the controller gains k and c as $k = \omega_n^2 + 2\zeta\omega_n/T = 9.54$ and $c = 2\zeta\omega_n + 1/T = 5.5$. The maximum angular rate is assumed as $|\omega_i|_{\max} = 10$ deg/s. The maximum control acceleration a_i is chosen as 40% of U/J_{ii} to accommodate the actuator dynamics, the nonlinear nature of quaternion-based phase-plane dynamics, and control acceleration uncertainty.

Figure 3 shows the time histories of attitude quaternions for the proposed three-axis control system but without employing the variable limiter. The sluggish response with excessive transient overshoot is evident for two successive, large-angle roll/pitch maneuvers. As shown in Fig. 4, the rapid multitarget acquisition and pointing capability of the proposed constant-gain control system with the variable limiter L is demonstrated. The angular rates are maintained within the specified limit of 10 deg/s, as can be seen in Fig. 5. Figure 6 shows the time histories of control input torques required to achieve such large-angle, rapid retargeting maneuvers.

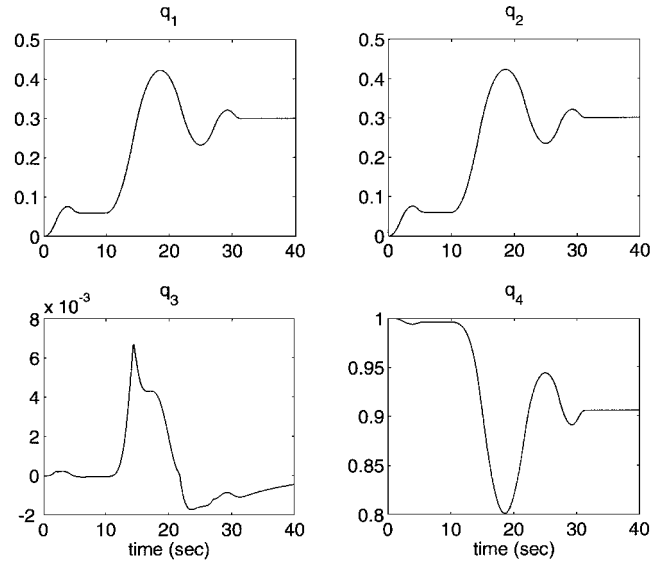

Fig. 3 Time histories of spacecraft attitude quaternions (constant-gain controller without variable limiter L).

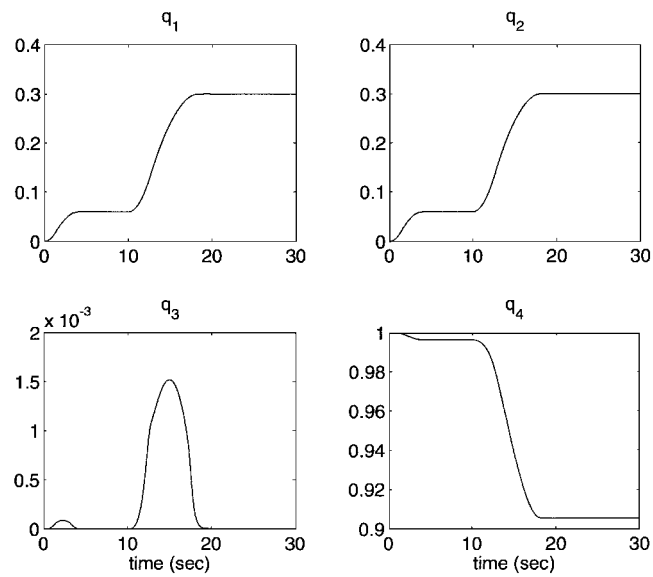

Fig. 4 Time histories of spacecraft attitude quaternions (constant-gain controller with variable limiter L).

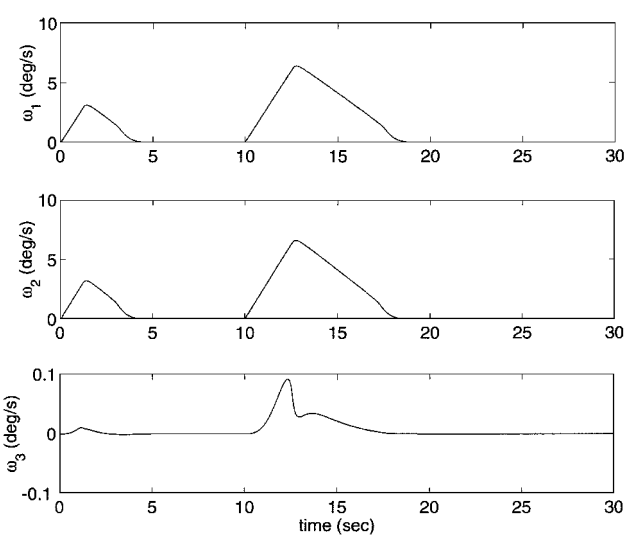

Fig. 5 Time histories of spacecraft angular rates (constant-gain controller with variable limiter L).

V. Agile Spacecraft Control Using CMGs

The proposed nonlinear feedback control logic is now applied to a more realistic problem of controlling an agile spacecraft using redundant single-gimbal CMGs. The control objective is to maneuver the spacecraft as fast as possible in the presence of the CMG internal singularities, momentum saturation, slew rate limit, and gimbal rate limits. Detailed discussions of a singularity problem inherent in a system of redundant single-gimbal CMGs can be found in the literature.[9–17]

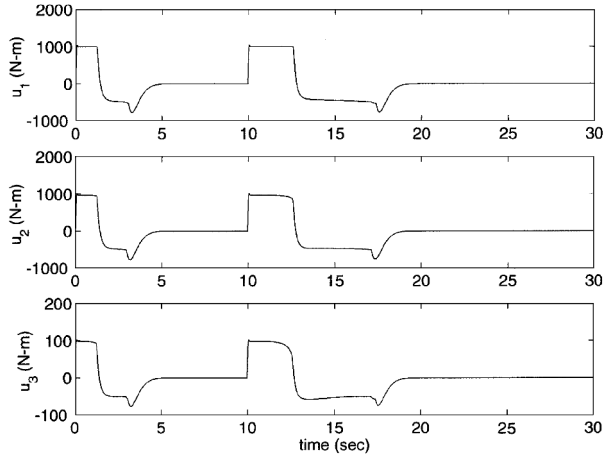

Fig. 6 Time histories of spacecraft control torques (constant-gain controller with variable limiter *L*).

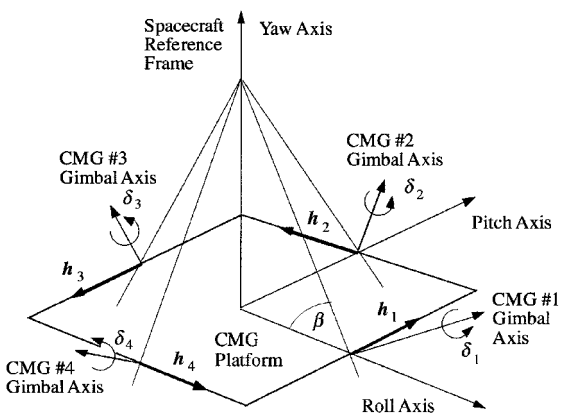

Fig. 7 Pyramid mounting arrangement of four single-gimbal CMGs.

A. Singe-Gimbal CMG Array and Pseudoinverse Steering Logic

Consider a typical pyramid mounting arrangement of four single-gimbal CMGs as shown in Fig. 7. A rigid spacecraft controlled by such CMGs is simply modeled as

$$\boldsymbol{J}\dot{\boldsymbol{\omega}} + \boldsymbol{\omega} \times \boldsymbol{J}\boldsymbol{\omega} = \boldsymbol{\tau} \tag{53a}$$

$$\dot{\boldsymbol{h}} + \boldsymbol{\omega} \times \boldsymbol{h} = -\boldsymbol{\tau} \tag{53b}$$

where $\boldsymbol{\tau}$ is the internal control torque vector generated by CMGs and $\boldsymbol{h}$ is the total CMG momentum vector. The CMG gimbal rate vector, $\dot{\boldsymbol{\delta}} = (\dot{\delta}_1, \dot{\delta}_2, \dot{\delta}_3, \dot{\delta}_4)$, is related to the CMG torque vector $\dot{\boldsymbol{h}}$ as follows:

$$\boldsymbol{A}\dot{\boldsymbol{\delta}} = \dot{\boldsymbol{h}} \tag{54}$$

where $\boldsymbol{A}$ is called the Jacobian matrix defined as

$$\boldsymbol{A} = \begin{bmatrix} -c\beta\cos\delta_1 & \sin\delta_2 & c\beta\cos\delta_3 & -\sin\delta_4 \\ -\sin\delta_1 & -c\beta\cos\delta_2 & \sin\delta_3 & c\beta\cos\delta_4 \\ s\beta\cos\delta_1 & s\beta\cos\delta_2 & s\beta\cos\delta_3 & s\beta\cos\delta_4 \end{bmatrix} \tag{55}$$

where $c\beta \equiv \cos\beta$, $s\beta \equiv \sin\beta$, and β is the skew angle shown in Fig. 7.

For a known spacecraft control torque input $\boldsymbol{\tau}$, the CMG momentum rate command or torque command $\dot{\boldsymbol{h}}$ can be chosen as

$$\dot{\boldsymbol{h}} \equiv \boldsymbol{u} = -\boldsymbol{\tau} - \boldsymbol{\omega} \times \boldsymbol{h} \tag{56}$$

and the gimbal rate command $\dot{\boldsymbol{\delta}}$ is then obtained as

$$\dot{\boldsymbol{\delta}} = \boldsymbol{A}^{+}\boldsymbol{u} \qquad \text{where} \qquad \boldsymbol{A}^{+} = \boldsymbol{A}^{T}(\boldsymbol{A}\boldsymbol{A}^{T})^{-1} \tag{57}$$

which is often referred to as the pseudoinverse steering logic. Most CMG steering laws determine the gimbal rate commands with some variant of pseudoinverse.

Most existing pseudoinverse-based, local inversion, or tangent methods, including the singularity robust (SR) inverse logic[18] of the form

$$\dot{\boldsymbol{\delta}} = \boldsymbol{A}^{+}\boldsymbol{u} \qquad \text{where} \qquad \boldsymbol{A}^{+} = \boldsymbol{A}^{T}(\boldsymbol{A}\boldsymbol{A}^{T} + \lambda\boldsymbol{I})^{-1} \tag{58}$$

do not always guarantee singularity avoidance and often unnecessarily constrain the operational momentum envelope of single-gimbal CMG systems. A single-gimbal CMG system with the SR inverse logic can become singular even in the presence of sensor noise. Furthermore, if it does become singular and a control torque is commanded along the singular direction, the system becomes trapped in the singular state because the SR inverse is unable to command nonzero gimbal rates.

B. Generalized SR Inverse

A simple yet effective way of passing through, and also escaping from, any internal singularities was developed recently in Refs. 19–21. The proposed logic is mainly intended for typical reorientation maneuvers in which precision pointing or tracking is not required during reorientation maneuvers, and it fully utilizes the available CMG momentum space in the presence of any singularities. Although there are special missions in which prescribed attitude trajectories are to be exactly tracked in the presence of internal singularities, most practical cases will require a tradeoff between robust singularity transit/escape and the resulting, transient pointing errors.

A CMG steering logic based on the generalized SR inverse[19–21] is simply given by

$$\dot{\boldsymbol{\delta}} = \boldsymbol{A}^{\#}\boldsymbol{u} \qquad \text{where} \qquad \boldsymbol{A}^{\#} = \boldsymbol{A}^{T}[\boldsymbol{A}\boldsymbol{A}^{T} + \lambda\boldsymbol{E}]^{-1} \tag{59}$$

and

$$\boldsymbol{E} = \begin{bmatrix} 1 & \epsilon_3 & \epsilon_2 \\ \epsilon_3 & 1 & \epsilon_1 \\ \epsilon_2 & \epsilon_1 & 1 \end{bmatrix} > 0 \tag{60}$$

The scalar λ and the off-diagonal elements ϵ_i are to be properly selected such that $\boldsymbol{A}^{\#}\boldsymbol{u} \neq 0$ for any nonzero constant $\boldsymbol{u}$.

Note that there exists always a null vector of $\boldsymbol{A}^{\#}$ because $\text{rank}(\boldsymbol{A}^{\#}) < 3$ for any λ and ϵ_i when the Jacobian matrix $\boldsymbol{A}$ is singular. Consequently, a simple way of guaranteeing that $\boldsymbol{A}^{\#}\boldsymbol{u} \neq 0$ for any nonzero constant $\boldsymbol{u}$ command is to continuously modulate ϵ_i, for example, as follows:

$$\epsilon_i = \epsilon_0 \sin(\omega t + \phi_i) \tag{61}$$

where the amplitude ϵ_0, the modulation frequency ω, and the phases ϕ_i need to be appropriately selected.[19–21]

It is emphasized that the generalized SR inverse is based on the mixed two-norm and weighted least-squares minimization, although the resulting effect is somewhat similar to that of artificially misaligning the commanded control torque vector from the singular vector directions. Because the proposed steering logic is based on the minimum two-norm, pseudoinverse solution, it does not explicitly avoid singularity encounter. Rather, it approaches and rapidly transits unavoidable singularities whenever needed. The proposed logic effectively generates deterministic dither signals when the system becomes near singular. Any internal singularities can be escaped for any nonzero constant torque commands using the proposed steering logic.

C. Simulation Results

The nonlinear feedback control logic developed in this paper is now integrated with the CMG steering logic based on the generalized SR inverse.[19–21]

A spacecraft with the following inertia matrix is considered:

$$\boldsymbol{J} = \begin{bmatrix} 21{,}400 & 2100 & 1800 \\ 2100 & 20{,}100 & 500 \\ 1800 & 500 & 5000 \end{bmatrix} \text{kg} \cdot \text{m}^2 \tag{62}$$

The yaw axis with the smallest moment of inertia is pointing toward a target.

Consider a typical pyramid mounting arrangement of four single-gimbal CMGs as shown in Fig. 7. A skew angle β of 53.13 deg (i.e., $\cos\beta = 0.6$, $\sin\beta = 0.8$) and 1000 N · m · s momentum magnitude for each CMG are assumed. The total maximum CMG momentum available then becomes 3200 N · m · s (not 4000 N · m · s) due to the pyramid mounting arrangement of four CMGs with $\beta = 53.13$ deg. The gimbal rate command limit of each CMG is assumed as 1 rad/s. It is also assumed that the attitude control bandwidth needs to be lower than 5 rad/s and the maximum slew rate less than 10 deg/s.

The proposed nonlinear attitude control system, consisting of the quaternion-errorfeedback control logic with the variable limiter and the CMG steering logic based on the generalized SR inverse $\boldsymbol{A}^{\#}$, is then described by

$$\boldsymbol{\tau} = -\boldsymbol{J}\left\{2k \operatorname*{sat}_{L_i}\left(\boldsymbol{e} + \frac{1}{T}\int \boldsymbol{e}\right) + c\boldsymbol{\omega}\right\} \tag{63a}$$

$$L_i = (c/2k)\min\left\{\sqrt{4a_i|e_i|},\ |\omega_i|_{\max}\right\} \tag{63b}$$

$$\boldsymbol{A}^{\#} = \boldsymbol{A}^T[\boldsymbol{A}\boldsymbol{A}^T + \lambda\boldsymbol{E}]^{-1} \tag{63c}$$

$$\boldsymbol{u} = -\boldsymbol{\tau} - \boldsymbol{\omega} \times \boldsymbol{h} \tag{63d}$$

$$\dot{\boldsymbol{\delta}}_c = \operatorname*{sat}_{\pm\dot{\delta}_{\max}}\{\boldsymbol{A}^{\#}\boldsymbol{u}\} \tag{63e}$$

$$\dot{\boldsymbol{\delta}} = \frac{(50)^2}{s^2 + 2(0.7)(50)s + (50)^2}\dot{\boldsymbol{\delta}}_c \tag{63f}$$

where $\dot{\delta}_{\max} = 1$ rad/s and $|\omega_i|_{\max} = 10$ deg/s. Similar to the numerical example in Sec. IV, if $\omega_n = 3$ rad/s, $\zeta = 0.9$, and $T = 10$ s, the controller gains k and c are chosen as $k = \omega_n^2 + 2\zeta\omega_n/T = 9.54$ and $c = 2\zeta\omega_n + 1/T = 5.5$. The maximum control acceleration a_i is chosen as 40% of U/J_{ii} to accommodate the actuator dynamics, nonlinear nature of quaternion kinematics, and control acceleration uncertainty.

For the normalized Jacobian matrix $\boldsymbol{A}$, the scale factor λ and $\boldsymbol{E}$ are chosen as

$$\lambda = 0.01\exp[-10\det(\boldsymbol{A}\boldsymbol{A}^T)] \tag{64a}$$

$$\boldsymbol{E} = \begin{bmatrix} 1 & \epsilon_3 & \epsilon_2 \\ \epsilon_3 & 1 & \epsilon_1 \\ \epsilon_2 & \epsilon_1 & 1 \end{bmatrix} \tag{64b}$$

where $\epsilon_i = 0.01\sin(0.5\pi t + \phi_i)$ with $\phi_1 = 0$, $\phi_2 = \pi/2$, and $\phi_3 = \pi$.

Simulation results for two successive, large-angle roll/pitch maneuvers are presented in Figs. 8–11. The rapid retargeting capability of the proposed nonlinear control system is demonstrated, as shown

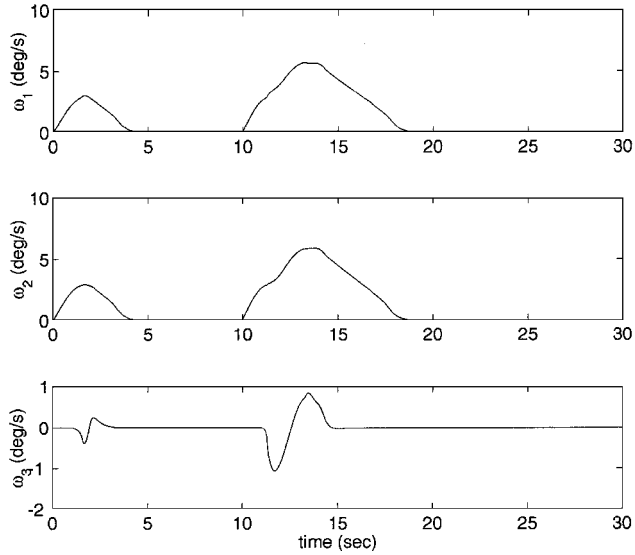

Fig. 9 Time histories of spacecraft angular rates (constant-gain controller with variable limiter L).

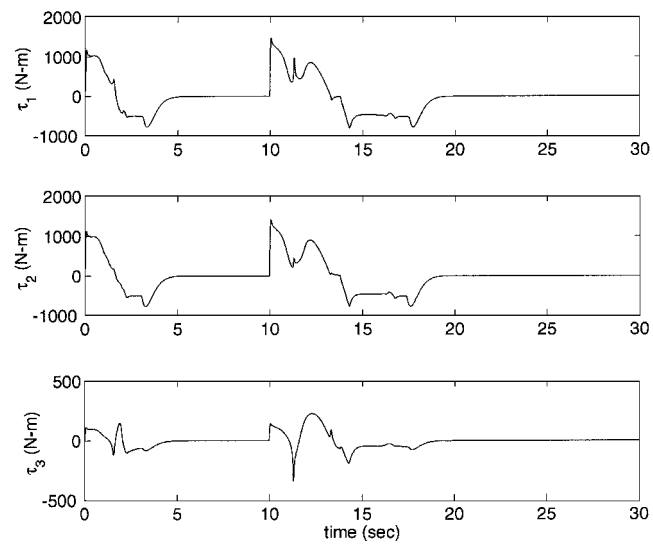

Fig. 10 Time histories of spacecraft control torques generated by CMGs (constant-gain controller with variable limiter L).

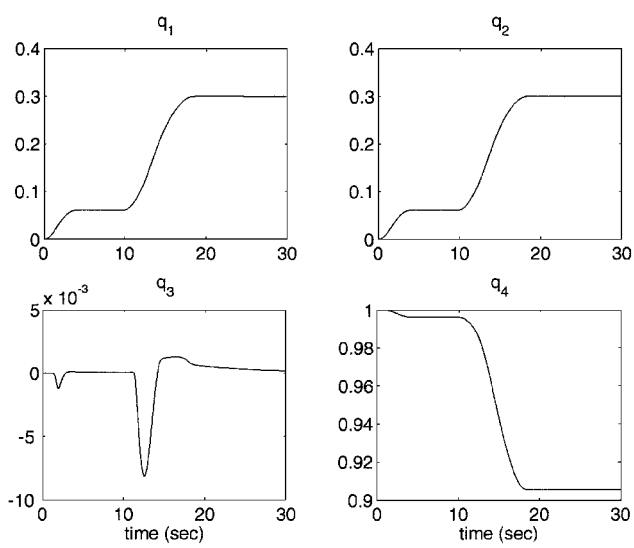

Fig. 8 Time histories of spacecraft attitude quaternions (constant-gain controller with variable limiter L).

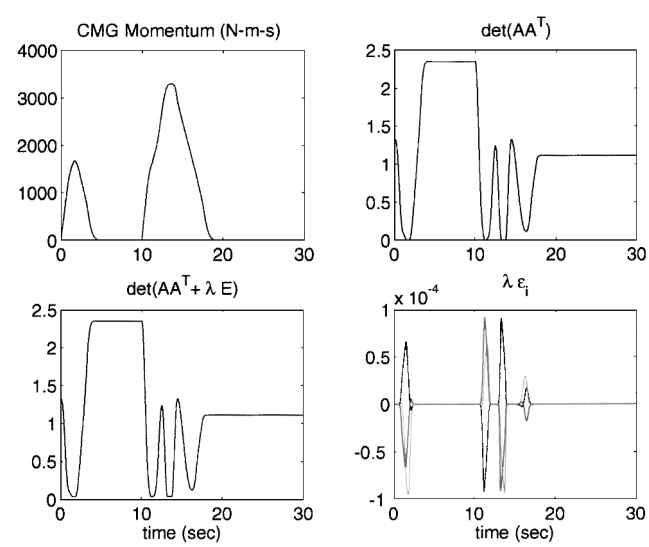

Fig. 11 Time histories of CMG momentum and singularity measures (constant-gain controller with variable limiter L).

in Fig. 8. Note that the overall responses shown in Figs. 8–10 for the case of spacecraft equipped CMGs are very similar to those in Figs. 4–6 for the generic three-axis control problem of Sec. IV. The time histories of CMG-generated control torques, shown in Fig. 10, are somewhat complex due to the CMG singularity problem.

The plots of the total CMG momentum and singularity measures, shown in Fig. 11, indicate that the CMG system with the proposed control logic successfully passed through the internal singularities and also utilizes the maximum CMG momentum of 3200 $N \cdot m \cdot s$ to achieve a rapid reorientation of the spacecraft. As can be seen in Fig. 11, the new CMG steering logic[19–21] does not explicitly avoid singularity encounters, but it rather approaches and rapidly transits the internal singularities whenever necessary.

In the next section, we will briefly discuss a more realistic case of pointing the line of sight of an imaging satellite in low Earth orbit toward multiple targets on the ground. This case was the main motivation for developing the proposed nonlinear control logic.

VI. Multiple Ground Target Tracking

A simulation study of the nonlinear attitude control system described in the preceding sections was performed for a realistic mission with many closely placed ground targets. A simple satellite configuration with the inertia matrix of $\boldsymbol{J} = \text{diag}(3400, 3400, 1200)$ $kg \cdot m^2$ was used. A regular six-sided pyramid arrangement of 100 $N \cdot m \cdot s$ CMGs was selected. The CMG gimbal axes have a skew angle of 65 deg from the roll/pitch plane. This produces an angular momentum ellipsoid with two equal major axes on the roll/pitch plane and a minor axis in the yaw direction. The lower angular momentum in the yaw direction still gives yaw approximately 20% more angular rate capability because of the small yaw inertia. This means that the mission planner can plan, based on line of sight (LOS), angle changes not accounting for the yaw component of the maneuver.

The orbit used in a simulation was 250 × 500 nm, inclined about 98 deg. Perigee occurs about one-third of the way through the simulation run. The distribution of sensor operations was a fixed distribution of the satellite maneuver angle. The location on the ground was such that when, including the time of maneuver, the orbital motion of the satellite and the rotation of the Earth would be from a distribution with more small angles, but still having some large-angle maneuvers. The location on the ground was not optimized in a minimum time order but rather a desired maneuvering load.

The measure of an agile satellite attitude control system is its ability to collect the maximum data from an area on the Earth that is rich in data collection opportunities. The planner selects the orientation of the satellite such that all data are scanned parallel to a latitude or longitude line. The scan was done in pure roll with respect to the Earth and in either direction. Each scan direction was selected such that the minimum yaw was needed for the maneuver and the scan direction continued in the direction of slew maneuver.

The schedule data transmitted to the satellite was latitude, longitude, altitude, and time for the beginning of scan and the end of scan. The control trajectory generator used the two points and the times to generate a constant rate trajectory that would pass through the two points. At the end of a scan (data collection) the commanded trajectory was stepped to the next scan trajectory. A particular simulation result is shown in Fig. 12.

The time to make a maneuver was not repeatable for a given change in LOS angle, but depended on the stored angular momentum in the CMG array, the direction of the maneuver, and the amount of yaw angle (not accounted for by the planner). The stored angular momentum was maintained at less than 10% of the total angular momentum, and, consequently, it was not a significant factor. Angular momentum determines the maneuver velocity. Saturation of angular momentum determined the velocity for large maneuvers and that the surface is not an ellipsoidal surface.

This complex problem of pointing the LOS of an imaging satellite in low Earth orbit toward multiple targets on the ground was the main motivation for developing the proposed nonlinear control logic. However, this paper is not intended to describe the details of this case.

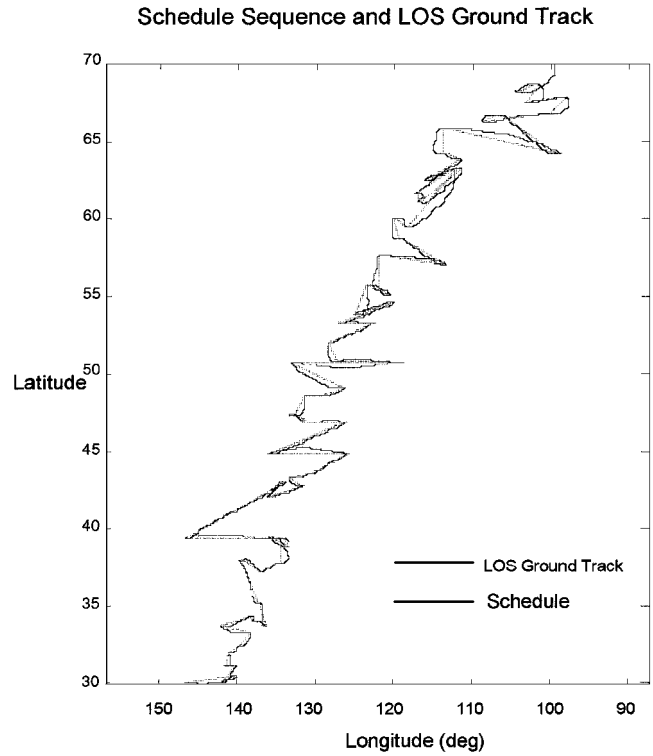

Fig. 12 Multiple ground target tracking simulation results.

VII. Conclusions

A nonlinear feedback control logic was developed for large-angle, rapid retargeting maneuvers subject to various physical constraints, such as the actuator saturation, slew rate limit, control bandwidth limit, etc. The proposed control logic utilized a variable limiter in the quaternion-error feedback loop. Simulation results for an agile spacecraft equipped with redundant single-gimbal control moment gyros demonstrated the rapid retargeting capability of the proposed nonlinear feedback control system. A more realistic case of pointing the LOS of an imaging satellite in low Earth orbit toward multiple targets on the ground was also briefly discussed.

Acknowledgments

The authors would like to thank the Reviewers and the Associate Editor, Alain Carrier, for their comments and suggestions for improving the quality of this paper.

References

[1]Wie, B., and Barba, P. M., "Quaternion Feedback for Spacecraft Large Angle Maneuvers," *Journal of Guidance, Control, and Dynamics*, Vol. 8, No. 3, 1985, pp. 360–365.

[2]Wie, B., Weiss, H., and Arapostathis, A., "Quaternion Feedback Regulator for Spacecraft Eigenaxis Rotations," *Journal of Guidance, Control, and Dynamics*, Vol. 12, No. 3, 1989, pp. 375–380.

[3]Wie, B., and Lu, J., "Feedback Control Logic for Spacecraft Eigenaxis Rotations Under Slew Rate and Control Constraints," *Journal of Guidance, Control, and Dynamics*, Vol. 18, No. 6, 1995, pp. 1372–1379.

[4]Wie, B., *Space Vehicle Dynamics and Control*, AIAA Education Series, AIAA, Reston, VA, 1998, Chap. 7.

[5]Bryson, A. E., Jr., and Ho, Y.-C., *Applied Optimal Control*, Hemisphere, Washington, DC, 1975, pp. 112, 113.

[6]Bailey, D., "Nonlinear Control of Velocity Limited Plants," U.S. Patent Pending, 1998.

[7]Franklin, G. F., Powell, J. D., Emami-Naeini, A., *Feedback Control of Dynamic Systems*, Addison–Wesley, Menlo Park, CA, 1994, pp. 196–199, 304–310.

[8]Friedland, B., *Advanced Control System Design*, Prentice–Hall, Englewood Cliffs, NJ, 1996, Chap. 6.

[9]Margulies, G., and Aubrun, J.-N., "Geometric Theory of Single-Gimbal Control Moment Gyro Systems," *Journal of Astronautical Sciences*, Vol. 26, No. 2, 1978, pp. 159–191.

[10]Bedrossian, N. S., Paradiso, J., Bergmann, E. V., and Rowell, D., "Steering Law Design for Redundant Single-Gimbal Control Moment

Gyroscopes," *Journal of Guidance, Control, and Dynamics*, Vol. 13, No. 6, 1990, pp. 1083–1089.

[11]Vadali, S. R., Oh, H., and Walker, S., "Preferred Gimbal Angles for Single-Gimbal Control Moment Gyroscopes," *Journal of Guidance, Control, and Dynamics*, Vol. 13, No. 6, 1990, pp. 1090–1095.

[12]Dzielski, J., Bergmann, E., Paradiso, J. A., Rowell, D., and Wormley, D., "Approach to Control Moment Gyroscope Steering Using Feedback Linearization," *Journal of Guidance, Control, and Dynamics*, Vol. 14, No. 1, 1991, pp. 96–106.

[13]Paradiso, J. A., "Global Steering of Single-Gimballed Control Moment Gyroscopes Using a Direct Search," *Journal of Guidance, Control, and Dynamics*, Vol. 15, No. 5, 1992, pp. 1236–1244.

[14]Kurokawa, H., "Constrained Steering Law of Pyramid-Type Control Moment Gyros and Ground Tests," *Journal of Guidance, Control, and Dynamics*, Vol. 20, No. 3, 1997, pp. 445–449.

[15]Schaub, H., and Junkins, J. L., "Singularity Avoidance Using Null Motion and Variable-Speed Control Moment Gyros," *Journal of Guidance, Control, and Dynamics*, Vol. 23, No. 1, 2000, pp. 11–16.

[16]Heiberg, C. J., Bailey, D., and Wie, B., "Precision Spacecraft Pointing Using Single-Gimbal Control Moment Gyros with Disturbance," *Journal of Guidance, Control, and Dynamics*, Vol. 23, No. 1, 2000, pp. 77–85.

[17]Ford, K. A., and Hall, C. D., "Singular Direction Avoidance Steering for Control Moment Gyros," *Journal of Guidance, Control, and Dynamics*, Vol. 23, No. 4, 2000, pp. 648–656.

[18]Nakamura, Y., and Hanafusa, H., "Inverse Kinematic Solutions with Singularity Robustness for Robot Manipulator Control," *Journal of Dynamic Systems, Measurement, and Control*, Vol. 108, Sept. 1986, pp. 163–171.

[19]Wie, B., Bailey, D., and Heiberg, C., "Singularity Robust Steering Logic for Redundant Single-Gimbal Control Moment Gyros," *Proceedings of AIAA Guidance, Navigation, and Control Conference* [CD-ROM], AIAA, Reston, VA, 2000; also *Journal of Guidance, Control, and Dynamics*, Vol. 24, No. 5, 2001, pp. 865–872.

[20]Wie, B., Bailey, D., and Heiberg, C., "Robust Singularity Avoidance in Satellite Attitude Control," U.S. Patent 6,039,290, 21 March 2000.

[21]Heiberg, C., Bailey, D., and Wie, B., "Continuous Attitude Control that Avoids CMG Array Singularities," U.S. Patent 6,131,056, 10 Oct. 2000.